ULTRASONIC BEAMS WITH BESSEL AND GAUSSIAN PROFILES

D. K. Hsu, F. J. Margetan, M. D. Hasselbusch,
S. J. Wormley, M. S. Hughes, and D. O. Thompson

Ames Laboratory
Iowa State University
Ames, IA 50011

INTRODUCTION

A novel technique has been developed for generating ultrasonic beams with spatial profiles of amplitude governed by a truncated Bessel function or Gaussian function [1,2]. Bessel beams have very unique properties; in optics Bessel beams have been shown to be diffractionless (J. Durnin et al, 1987 [3,4]). In a related work, R. W. Ziolkowski et al [5] reported experimental measurements of "acoustic directed energy pulse trains" generated by synthetic line array of ultrasonic transmitters in water. However, a Bessel function ultrasonic transducer has never been reported before. Gaussian beams also have desirable properties; they are very easy to model analytically, and a circular Gaussian function ultrasonic transducer is free of near-field nulls and far-field sidelobes associated with conventional "piston source" transducers [6]. At least three designs of Gaussian transducers have been reported in the literature in the past 30 years [7-9]. We report a method in which piezoelectric ceramic elements are poled with nonuniform electric fields shaped like Bessel or Gaussian functions such that the resulting polarization (and hence the ultrasonic amplitude) follows that of the applied poling field. Like conventional piston source transducers, such Bessel or Gaussian transducers also possess the simple "parallel plate capacitor" configuration and can be packaged likewise. Beam profiles and propagation behavior of these Bessel and Gaussian transducers have been measured experimentally in an immersion tank and the results compared well with model predictions

NONUNIFORM POLING OF PIEZOELECTRIC CERAMICS

In order to pole a piezoelectric element with an electric field of the form of a (truncated) Gaussian or Bessel function, such a field must first be generated. One way to produced nonuniform electric fields is to use shaped electrodes. However, the piezoelectric material used (PZT-5A) has an extremely high relative dielectric constant (about 1700 after poling); as a result, almost all the applied poling voltage will drop across any small gap between the PZT and the electrodes instead of in the PZT. Hence, the required electrode shape for the Gaussian field or Bessel field is machined into the PZT and the metallization is applied directly on the surface of the PZT to eliminate any gaps. The machining of hemispherical cavities into PZT is not difficult and can be done with ball cutters covered with surface abrasive particles using water as a lubricant on common machine shop equipment.

Review of Progress in Quantitative Nondestructive Evaluation, Vol. 9
Edited by D.O. Thompson and D.E. Chimenti
Plenum Press, New York, 1990

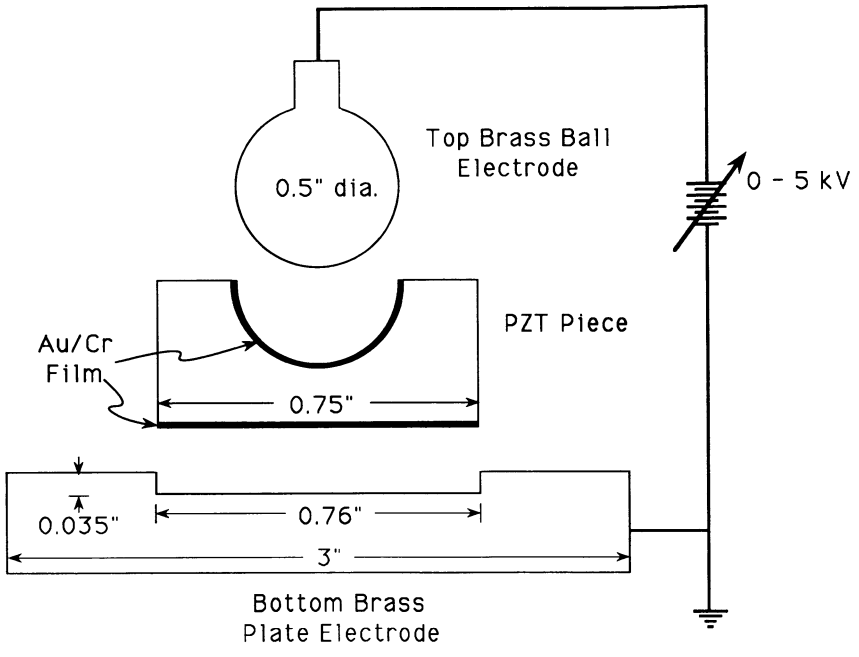

Fig. 1 Electrode configuration for poling the shaped PZT disk with a Gaussian profile.

Figure 1 shows poling arrangement for the Gaussian transducer. The top surface of a PZT disk (0.75" diameter and 0.298" thick) is machined to contain a hemispherical cavity of 0.25" radius so that the thinnest point of the disk is 0.048". The surface of the cavity and the bottom surface of the PZT disk are evaporated with gold-over-chromium films. The poling is done in diffusion pump oil at a temperature of $95^{o} \pm 2^{o}C$ with an applied voltage of 3700 volts. The voltage is held for 4 minutes and then removed. After poling, the top portion with the cavity is cut off with a low speed diamond wafer saw to leave a circular disk 0.035" thick. This thickness correponds to the fundamental longitudinal mode with a frequency of 2.25 MHz. The cut surface is then evaporated again with gold-over-chromium film. The Gaussian transducer element, now in the form of a flat and parallel disk with full electrode plating on both faces, is then mounted in a metal case for immersion measurements of its ultrasonic field profile. The transducer is driven by a negative spike pulse of -175 volts from a Panametics 5052 pulser/receiver. Both backed and unbacked transducers have been made; the unbacked transducer produces essentially a toneburst at 2.25 MHz and its field profile can thus be compared conveniently with the calculated profile for a single frequency [1].

The poling of the Bessel function transducer is similar to that of the Gaussian transducer. Figure 2 shows the poling of a three-lobe Bessel transducer. To produce a permanent polarization patterned after the amplitude and phase of a truncated Bessel function $J_0(r)$, one must polarize different parts of the disk with electric fields of different intensity as well as polarity, as shown in Fig. 2. A 1" diameter 0.219" thick PZT-5A is machined with a central cavity and two concentric ring grooves. The location and depths are chosen to correspond with the spacing and amplitude of the Bessel function $J_0(r)$. After poling the "scalloped" top part of the disk is cut off to leave a 0.035" thick flat and parallel disk, and both faces of the disk are then evaporated with full metallization. The unbacked transducer element is mounted in a metal can for immersion measurements of its ultrasonic field profile [2].

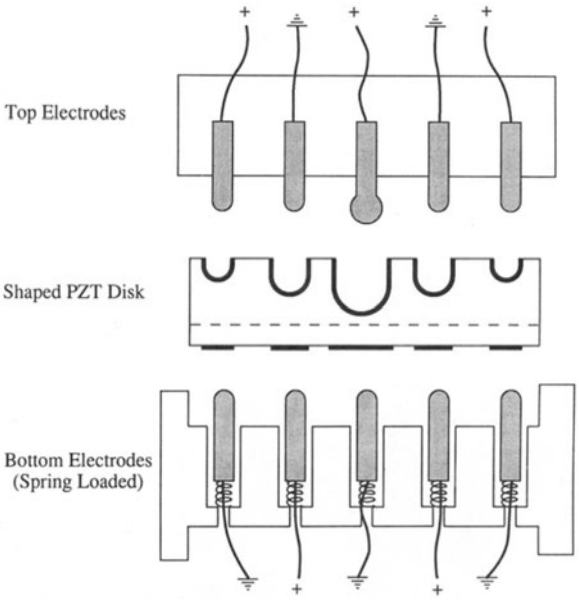

Fig. 2. Electrode configuration and polarity for poling a three-lobe Bessel transducer.

FIELD PROFILE OF GAUSSIAN TRANSDUCER

Consider a circular transducer vibrating harmonically in the longitudinal (thickness) mode with an amplitude across its face described by a Gaussian function. The Gaussian amplitude profile centered at the center of the transducer has a 1/e halfwidth of W(0) at the face of the transducer and a 1/e halfwidth of W(z) at a propagation distance z along its axis. Then, the magnitude of the displacement or pressure field U(x,y,z) produced by the Gaussian transducer can be written as

$$U(x,y,z) = A\,[W(0)/W(z)]\,\exp[-(x^2 + y^2)/W^2(z)] \qquad (1)$$

where

$$W(z) = [\lambda/\pi W(0)](z^2 + \pi^2 W^4(0)/\lambda^2)^{1/2}$$

Here A is a strength factor dependent upon the driving voltage and the electromechanical coefficient of the transducer material and λ is the wavelength of the propagating wave in the isotropic medium the transducer is radiating into.

This equation describes both the axial and the radial changes of the Gaussian beam as it propagates in the medium. It can therefore be programmed into a computer for the rapid generation of beam profiles based on four parameters: the maximum amplitude of oscillation A at the face of the transducer, the 1/e halfwidth W(0) at the face of the transducer, the frequency of oscillation and the speed of sound in the medium. In this work, such theoretical beam profiles were generated to compare with the experimentally measured beam profiles.

Experimentally the field amplitudes produced by the nonuniformly poled Gaussian transducer were measured in a water immersion tank with a point probe having a diameter of 0.025 cm. Data were collected in a plane perpendicular to the face of the transducer and containing the center of the transducer. Since the transducer has axial symmetry, field

scan in this plane determines the spatial field profile completely. A rastered scan of 51 points in the lateral direction at 17 different distances from the transducer was made.

Figure 3(a) shows a 3D plot of the measured field profile of the Gaussian transducer. In the lateral direction there are 51 points to a line and the spacing between adjacent points is 0.025". The lateral scan therefore covers a distance of 1.25" centered with respect to the 0.75" diameter transducer. In the axial direction there are 17 lines with a spacing between adjacent lines of 0.5". The scan covers an axial distance from 0.75" to 8.75". The vertical axis of the plot shows the amplitude of the signal in volts. The 1/e halfwidth of the first scan line at 0.75" is 0.189". As can be seen, there are no nearfield nulls even though the signal has a very narrow frequency bandwidth (Q = 13).

In order to compare the experimental results in Fig. 3(a) with model prediction, Eq. (1) was used to compute the theoretical beam profile based on the following parameters. The amplitude A at the face of the transducer was chosen such that the on-axis amplitude at large distance (8.75") agreed with the measured result. The 1/e halfwidth W(0)

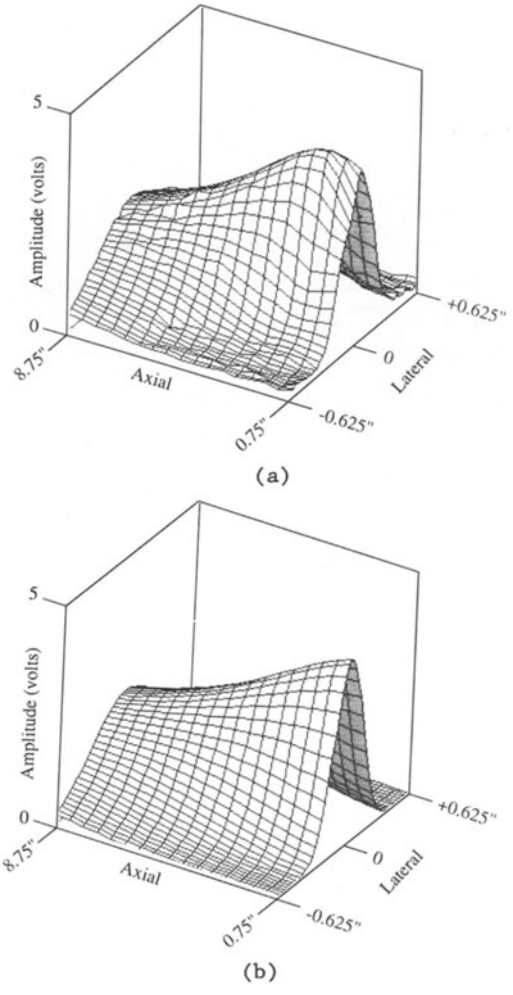

Fig. 3. (a) Experimentally measured field profile of the Gaussian transducer. (b) Theoretically computed Gaussian field profile using Eq. (1).

at the face of the transducer was chosen to be 0.186" so as to reproduce the measured 1/e halfwidth of 0.189" at z = 0.75". A frequency of 2.25 MHz and a speed of sound in water of 0.148 cm/μs were used in the calculation. The calculated beam profile, to be compared directly with the results in Fig. 3(a), is shown in Fig. 3(b). As can be seen, the quantitative agreement between experiment and theory is quite good. It should also be pointed out that the 1/e halfwidth of the ultrasonic field at the face of the transducer, W(0) = 0.186", deduced in fitting the experimental data to the model, is quite close to the 1/e halfwidth 0.196" of the electric field profile used in the poling of the transducer.

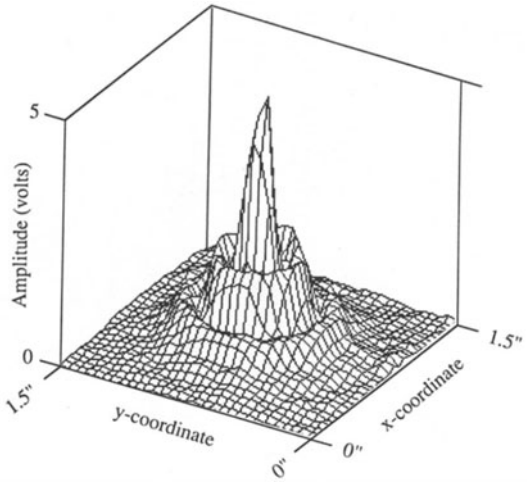

Fig. 4. Ultrasonic field magnitude profile of the 1" diameter, 2.25 MHz, three-lobe Bessel transducer in a plane 1.12" from the surface.

FIELD PROFILE OF BESSEL TRANSDUCER

The ultrasonic radiation field produced by the Bessel transducer was also mapped out in water using the same point probe receiver. Initial scans were performed to examine the degree of axial symmetry. The result of one such scan, depicting the received voltage magnitude as a function of the transverse coordinates x and y, is shown in Fig. 4. The scan was conducted in a plane parallel to the face of the transducer and at a distance of 1.12" from it. The voltage signal output of the point probe was proportional to the local particle displacement field. Thus Fig. 4 essentially represents a "bird's eye view" of the particle displacement magnitude in water with the Bessel transducer aimed vertically upward. The field possesses a high degree of symmetry and the three lobes of the Bessel profile can be easily seen. When the rf waveforms were examined to study the phase behavior, the central lobe and the second lobe regions of the transducer were observed to vibrate out of phase with the first lobe, as expected in a Bessel field.

Since the field pattern was axially symmetric, the full three dimensional beam profile could be ascertained by conducting a two-dimensional scan in a plane perpendicular to the face of the transducer and containing the symmetry axis (z) of the transducer disk.

Such a scan was made using the point probe, covering an axial range of $0.125" \leq z \leq 9.125"$ and a lateral range of $-0.775" \leq z \leq 0.775"$. The received voltage magnitude is displayed in Fig. 5(a). Again, the lobes are well defined. For comparison, the theoretically calculated beam profile (using a Gauss-Hermite model [10]) for an ideal 1" diameter, 2.25 MHz, three-lobe, truncated Bessel transducer is shown in Fig. 5(b). The agreement between the measured and calculated fields is seen to be quite good.

We now turn to the "diffractionless" feature of a Bessel beam. An examination of Fig. 5 shows that the three-lobe Bessel transducer driven at 2.25 MHz exhibited considerable diffraction (beam spreading and amplitude drop-off). However, the same transducer exhibited much less diffraction when it was excited to generate ultrasonic waves at its higher harmonics. One way to quantify the degree of diffraction is to examine the "range" in water of a propagating beam. Here we define the range R as the axial distance at which the on-axis amplitude of the

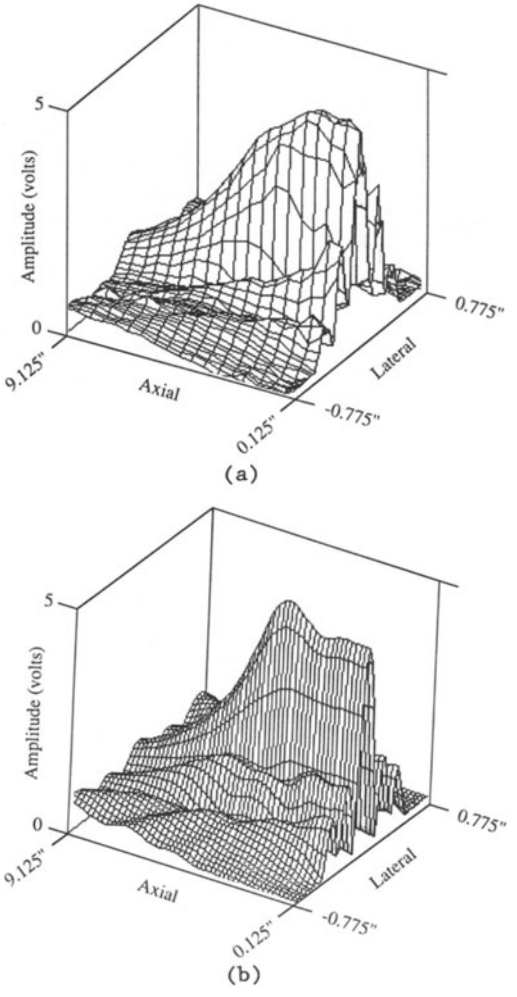

Fig. 5. (a) Experimentally measured ultrasonic field magnitude profile of the Bessel transducer. (b) Computed results using the Gauss-Hermite beam model

ultrasonic displacement dropped to one half of the amplitude at the transducer face. Computer simulations using the Gauss-Hermite model were conducted to determine the range in water of an ultrasonic beam produced by an ideal, truncated, Bessel transducer. The range was found to depend upon the vibrating frequency (f), the number of lobes (n) and the radius (a) of the transducer. Ignoring the attenuation of ultrasound in water, it was found that the range of a truncated Bessel transducer could be written as:

$$R \approx 15.8 \; f \; a^2/n \tag{2}$$

where f is frequency in MHz and range R and radius a are in centimeters. Figure 6 shows a comparison between the Bessel probe range for various (f, n, a) combinations computed by the Gauss-Hermite model and predicted by the empirical formula Eq. (2). If the agreement were perfect, all the points in Fig. 6 would fall on the solid straight line.

For the Bessel function $J_0(r)$, with the exception of the central lobe, the distances between adjacent zero crossings are approximately constant. Defining this distance as the lobe width w, we have $a \approx nw$ for large n. The empirical formula Eq. (2) for large n can therefore be written as:

$$R \approx 15.8 (f \, n \, w^2), \tag{3}$$

with the frequency f in MHz and the range R and lobe width w in centimeters. The difference between the ranges predicted by Eqs. (2) and (3) is generally less than 10% for n>5 and decreases rapidly with increasing n. Based on Eq. (3), one can conclude that a large range (or low diffraction) can be achieved with a large Bessel transducer (large number of lobes and large lobe width) operated at high frequencies. For example, the range of a five-lobe Bessel transducer with a lobe width of 0.4 cm (about 4 cm total diameter) would be approximately 126 cm at 10 MHz, discounting attenuation in water. It is important to realize that low diffraction can be achieved only by having both a large n and a large

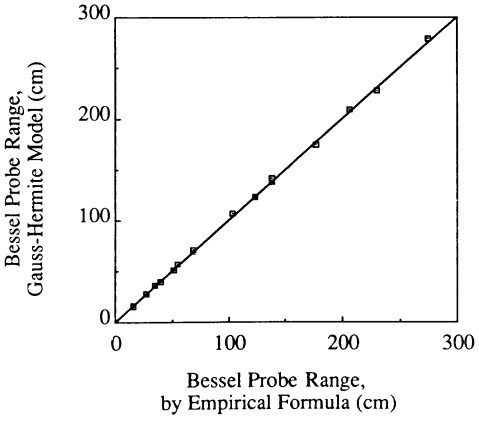

Fig. 6. Comparison of the Bessel transducer range computed using the Gauss-Hermite model and using the empirical formula Eq. (2).

w. For a Bessel transducer of a given total size, increasing the number of lobes it contains actually decreases the range because the square of the lobe width decreases faster than n increases.

CONCLUSION

A novel technique has been developed to polarize piezoelectric ceramic transducers nonuniformly and thereby build the desired field profile into the transducer. Both Gaussian function and Bessel function transducers have been built with this method and the measured field profiles agreed well with the calculated profiles. This transducer fabrication method produces flat and parallel circular disk elements with the usual full-plating electrode configuration. They can therefore be backed and packaged like conventional transducers.

ACKNOWLEDGEMENT

The authors wish to thank G. J. Posakony of Battelle Northwest for supplying the point probe and Byron Newberry for useful discussions on beam modeling. This work was supported by the Director for Energy Research, Office of Basic Energy Sciences of the U. S. Department of Energy under Contract No. W-7405-ENG-82.

REFERENCES

1. D. K. Hsu, F. J. Margetan and D. O. Thompson, "Bessel Beam Ultrasonic Transducer: Fabrication Method and Experimental Results", submitted to Applied Physics Letters.
2. D. K. Hsu, F. J. Margetan, M. D. Hasselbusch, S. J. Wormley, M. S. Hughes, and D. O. Thompson, "Technique for Nonuniform Poling of Piezoelectric Element and Fabrication of Gaussian Transducers", submitted to IEEE Transactions on Ultrasonics, Ferroelectrics and Frequency Control.
3. J. Durnin, J. Opt. Soc. Am. A4, 651 (1987).
4. J. Durnin, J. J. Miceli and J. H. Eberly, "Diffraction-Free Beams", Phys. Rev. Lett., 58(15), 1499-1501 (1987).
5. R. W. Ziolkowski, D. K. Lewis and B. D. Cook, "Evidence of Localized Wave Transmission", Phys. Rev. Lett., 62(2), 147- 150 (1989).
6. W. Sachse and N. N. Hsu, "Ultrasonic Transducer for Materials Testing and their Characterization", in Physical Acoustics Vol. XIV, edited by W. P. Mason and R. N. Thurston, (Academic Press, New York, 1979). pp. 277-406.
7 K. V. Haselberg and J. Krautkramer, "Ein Ultraschall- Strahler fur die Werkstoffprufung mit Verbessertem Nahfeld", Acoustica 9, 359-364 (1959).
8. F. D. Martin and M. A. Breazeale, "A Simple Way to Eliminate Diffraction Lobes Emitted by Ultrasonic Transducers", J. Acoust. Soc. Am. 49, 1668-1669 (1971).
9. R. O. Claus and P.S. Zerwekh, "Ultrasonic Transducer with a Two-Dimensional Gaussian Field Profile", IEEE Trans. Sonics and Ultrasonics, 30, 36-39 (1983).
10. R. B. Thompson, T. A. Gray, J. H. Rose, V. G. Kogan and E. F. Lopes, "The Radiation of Elliptical and Bi-cylindrically Focused Piston Transducers", J. Acoust. Soc. Am., 82, 1818- 1828 (1987).